ANNALES
UNIVERSITATIS MARIAE CURIE-SKŁODOWSKA
LUBLIN – POLONIA
VOL. LXII, 5 SECTIO AA 2007

Determination of reduction mechanism by TPR data for $FeO-H_2$ system

W. K. Jóźwiak, E. Kaczmarek, W. Ignaczak
Institute of General and Ecological Chemistry, Technical University of Łódź, Żeromskiego 116, 90-924 Łódź, Poland, e-mail: wjozwiak@.p.lodz.pl

Reduction behaviour of iron (II) oxide (wüstite) was characterized by applying temperature programmed reduction in 5% H_2 – 95% Ar gaseous stream. The experimental TPR_{H2} data fit well to Avrami-Erofeev models with self-catalyzed nucleation rate-determining steps. For low heating rates, up to 1 °C/min, reduction of FeO to Fe occurs *via* three-dimensional nucleation model, whereas for higher heating rates, reduction can be described by two-dimensional nucleation model. Instead of one simple reduction reaction FeO to Fe the competitive, more complex pathway FeO to Fe_3O_4 to Fe should be reconsidered as a result of temperature activated wüstite disproportionation 4FeO to Fe_3O_4 plus Fe below 579 °C. Both, the metallic iron self-catalyzed nucleation combined with dissociative chemisorption of hydrogen molecules and hydrogen atoms spillover into reduction interface region Fe/FeO and/or FeO disproportionation regions Fe_3O_4/Fe/FeO can be crucial. The activation energy, E = 112 kJ/mol can be determined independently of the assumed reduction mechanism.

1. INTRODUCTION

Temperature-Programmed Reduction method (TPR) has been widely applied to obtain qualitative characterization of solid materials [1-5]. A considerable interest has been focused on the reducibility of bulk iron oxides [6] and iron oxides dispersed on different supports as well [7]. The reduction process of iron (III) oxides to Fe metal was examined generally in the isothermal mode or TPR conditions. However, it must be taken into account that there are considerable differences in regard of, for example, the choice of reduction temperature, water partial pressure and crystallite size of powdered samples. Most of the literature

references concerned mainly the reduction of Fe_2O_3 to Fe_3O_4 and Fe_2O_3 or Fe_3O_4 to Fe. Using Fe_2O_3 as a starting material usually a two-step reduction was observed, namely pre-reduction of Fe_2O_3 to Fe_3O_4 as an intermediate and then final reduction of Fe_3O_4 to metallic Fe, which can be described by the following scheme:

$$Fe_2O_3 \rightarrow Fe_3O_4 \rightarrow Fe \qquad (a)$$

A three-step reduction pathway involving both Fe_3O_4 and FeO as intermediates is often postulated [8]:

$$Fe_2O_3 \rightarrow Fe_3O_4 \rightarrow FeO \rightarrow Fe \qquad (b)$$

Although FeO phase is thermodynamically unstable iron (II) oxide below 570 °C [7,9] has often been considered as an intermediate compound. Wüstite belongs to so called nonstoichiometric compounds $Fe_{1-x}O$ where ($0.83 < 1-x < 0.95$) for p = 0.1 MPa, T > 567 °C [9]. The appearance of wüstite-like phase involved in the reduction process of many oxy and/or hydroxy Fe(III) compounds usually was not confirmed experimentally. On the other hand a rather exceptional appearance of wüstite phase among final products of iron (III) oxide reduction is claimed on the basis of Mösbauer spectroscopy or TPR_{H2} measurements of both supported and unsupported iron oxides [7,8]. The main reason for our attention focused on the temperature programmed reduction behavior of wüstite in hydrogen atmosphere resulted from the lack of general acceptance of FeO as an intermediate of iron (III) oxides reduction and the fact that reduction behavior of FeO alone to Fe, in hydrogen atmosphere in temperature range below 700 °C has not been the subject of common interest.

2. EXPERIMENTAL

As an investigated material, thermodynamically meta-stable wüstite compound, purchased from Aldrich firm (FeO – 99.99 % purity) was used.

Determination of the surface area: Specific surface area was measured by BET (liquid N_2) method. Taking into account surface area of FeO (below 1 m^2/g) and assuming that all particles are spherical, nonporous and have identical size the average particle diameter can be anticipated as 1.2 μm. On the basis of XRD data the average FeO particle size about 130 nm was estimated. After hydrogen reduction the average diameter of Fe metallic particles was about 36 nm.

Temperature programmed reduction TPR_{H2} measurements were carried out in a conventional apparatus. The TPR reactor was a quartz tube with internal diameter 5 mm. A reducing mixture 5% H_2 – 95% Ar with flow rate 40 cm^3/min. was applied. The hydrogen concentration in gaseous mixture was measured by thermal conductivity detector. A dry ice/acetone trap – bath was used to freeze away water produced during the reduction process. In all experiments sample weight of about 10 mg was used. The linear temperature heating rates: 0.58, 1.07, 2.57, 5.52 and 10.7 °C/min. from room temperature up to 700°C were applied for all TPR measurements. The selection of appropriate conditions to avoid any mass transfer limitations for TPR measurements has been checked on the basis of literature criterions [10,11]. Quantitative TPR analysis pointed out that the reproducibility of TPR measurements was in the range ±10%. For TPR calibration copper (II) oxide sample was used as a standard.

It this work was found that for study reduction process of wüstite the Avarmi–Erofeev's reduction models concerning the nucleation process from the statistical probability treatment [2, 12, 14-17] could be used. Appropriate forms of the f(α) and g(α) functions of these reduction models are given in Table 1.

Tab. 1. The f(α) and g(α) function of different reduction models

Reduction model	f(α)	g(α)[a]
Three-dimensional nucleation according to Avarmi-Erofeev	$(1-\alpha)(-3\ln(1-\alpha))^{2/3}$	$(-3\ln(1-\alpha))^{1/3}$
Two-dimensional nucleation according to Avarmi-Erofeev	$(1-\alpha)(-2\ln(1-\alpha))^{1/2}$	$(-2\ln(1-\alpha))^{1/2}$

where $^{a}g(\alpha) = \int_0^{\alpha} \frac{d\alpha}{f(\alpha)}$

3. RESULTS AND DISCUSSION

The influence of heating rate on TPR profiles of FeO under the same experimental conditions is presented in Figure 1 and one can see the shift of TPR peaks to higher temperatures with an increasing heating rate. For the heating rates 0.58, 1.07, 2,57, 5.52, and 10.7 °C/min the temperature maximum peaks was equal: 393; 422; 442; 460; and 500 °C, respectively.

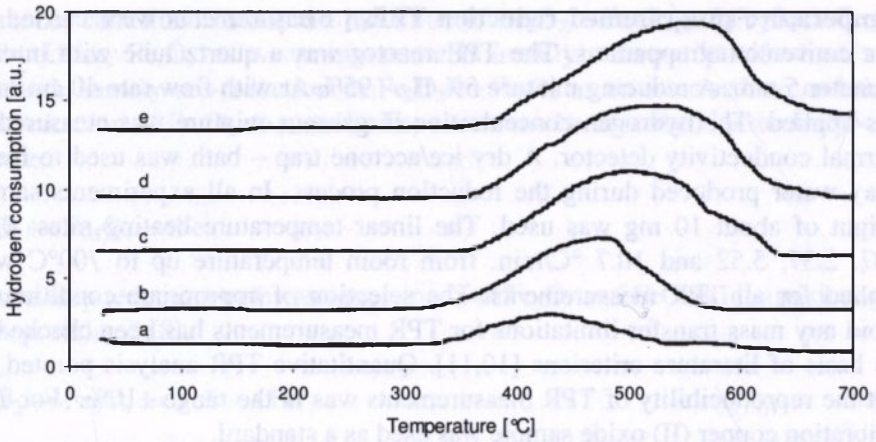

Fig.1. The influence of linear heating rate on TPR_{H2} profiles of iron (II) oxide samples: curves a, b, c, d and e for heating rates φ [°C/min]: 0.58, 1.07, 2.57, 5.52, 10.7, respectively. FeO sample mass: 0.01g, in all experimental runs.

Taking into account that both FeO is thermodynamically stable above 570 °C and the fact that the disproportionation reaction of FeO takes place in the temperature range 250–600 °C [18]:

$$4FeO \rightarrow Fe_3O_4 + Fe \qquad (c)$$

instead of one simple equation of the equivalent FeO reduction:

$$4(FeO + H_2 \rightarrow Fe + H_2O) \qquad (d)$$

one can expect an additional accompanying one-step reduction of Fe_3O_4, below 570°C:

$$Fe_3O_4 + 4H_2 \rightarrow 3Fe + 4H_2O \qquad (e)$$

or even, gradual - two step reduction of Fe_3O_4, if its temperature range overlaps 570 °C:

$$Fe_3O_4 + H_2 \rightarrow 3FeO + H_2O \qquad (f)$$

$$3(FeO + H_2 \rightarrow Fe + H_2O) \qquad (g)$$

The disproportionation of FeO, equation (c) reflects both the formation of metallic iron phase ($Fe^{2+} \rightarrow Fe^0$) and the formation of a stoichiometrical amount

of magnetite phase ($3Fe^{2+} \rightarrow 2Fe^{3+} + Fe^{2+}$). This redox reaction was confirmed by *'in situ"* XRD method of FeO reduction, not only in the reductive atmosphere of hydrogen or carbon monoxide, but also in the neutral atmosphere of argon. The disproportionation reaction of FeO (c) starts above 200 °C and not consuming hydrogen is much easier than FeO reduction reaction occurring above 350 °C (d–f). The main reason seems to result from different mechanistic pathways of disproportionation and reduction reactions. The disproportionation, three solid phases reaction: wüstite ↔ magnetite + iron (c) makes apparently simpler two solids-wüstite reduction FeO → Fe (d) a more complicated process (d–f). In the case of thermodynamically forced, FeO disproportionation, the oxygen atom sub-lattice of crystal network does not change very much during wüstite → magnetite transformation and only the process of metallic iron phase nucleation requires temperature activated diffusion of iron atoms into inter-phase FeO/Fe_3O_4 region. The lack of symmetry of hydrogen peak was observed especially when heating rates higher than 1.07 °C/min. were applied (curves c–e in Figure 1) and it can be assigned to relatively easy nucleation, equation (c), reflected on the low temperature side of TPR peak and the change of FeO reduction mechanism located at about 570 °C of temperature – the high temperature side of TPR peaks, equations (e–g). Thus, depending on the heating rate the simple one-step reduction FeO → Fe can be treated as a much more complicated two-step process FeO → Fe_3O_4 → Fe up to 570 °C, or even a three-step process FeO → Fe_3O_4 → FeO → Fe above 570 °C. Such an approach would rationalize the existence of different iron oxides, Fe_3O_4, FeO as intermediates not depending very much on the kind of starting iron oxide, but mostly dependent on reduction temperature determining entirely the reduction mechanistic pathways [18].

The degree of FeO reduction (α) was determined from the analysis of TPR profile. To get this goal surface area of TPR peak was divided into very small parts (rectangles), for instance 100 ones, using a computer technique resulting in their total surface area is being approximately equal the total surface area under TPR peak. It was assumed that each of these small surface areas can express fraction conversion (α).

In Figure 2 the degree of reduction (α) as a function of time is represented by S-shaped curves characteristic of the applied heating rate. Using chosen (α) values, recommended by lit. [19] namely, $0.05 < \alpha < 0.9$, in this case, the very first step of iron phase nucleation and last stages of FeO (or rather Fe_3O_4) reduction are omitted, can observe on linearity of appropriate g(α) function vs. time for the established reduction model. The differential form of the Avrami-Erofeev's equation [12] is as follows:

$$\frac{d\alpha}{dt} = nk^{1/n}\left[-\ln(1-\alpha)^{1-1/n}\right](1-\alpha) \qquad (1)$$

where: the exponent $n = \beta + \lambda$, and β is the number of steps involved in nucleolus creation, often $\beta = 1$ or 0, the latter describing instantaneous nucleation, and λ is the number of dimensions in which the nuclei grow, and so, $\lambda = 1$ for linear, 2 for discs or cylinders, 3 for spheres or hemispheres development. The obtained results are presented in Figures 3-4 for 3-D and 2-D nucleation models, respectively.

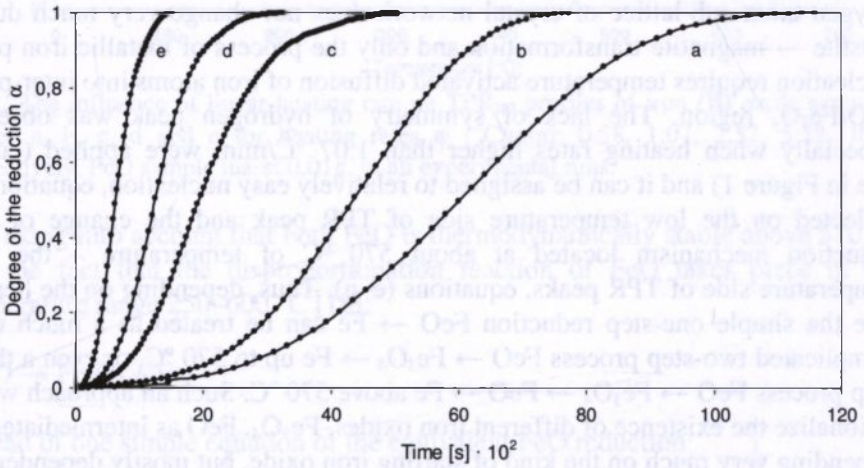

Fig. 2. Degree of the reduction α vs. time [s], curves a-e for different linear heating rate φ: 0.58, 1.07, 2.57, 5.52 and 10.7 °C/min, respectively.

Figure 3 shows graphs of the $g(\alpha)$ function vs.time for the 3-D and 2-D-dimensional nucleation model for low heating rates, 0.58 and 1.07 °C/min. and higher heating rates, 2.57, 5.52, and 10.7 °C/min for FeO reduction to metallic Fe. It can be seen that TPR data fit well into those nucleation models (correlation factor R^2 of perfect straight lines in Figure 3 is very nearly equal to unity). Assuming instantaneous nucleation, namely $\beta = 0$ and $\lambda = 3$, for the 3-D nucleation model, can indicate the formation of nuclei throughout the particles, followed by a linear growth of the nuclei in three dimensions, including the overlap of growing nuclei. Similarly, for 2-D nucleation, assuming instantaneous nucleation, this is, $\beta = 0$ and taking into consideration that $\lambda = 2$, the formation of interface nuclei is followed by its linear growth in two directions. Thus, the higher heating rate reduction, via 2-D surface reduction of FeO to Fe (or rather Fe_3O_4 to FeO and finally to Fe), predominate over the lower heating rate

reduction via 3-D volume reduction. One can see in Figures 1 and 2 the occurrence of an induction period, which according to literature [20] is associated with nucleation process as the rate-determining step in a uniform internal reduction. The shift of the FeO → Fe reduction peak which is shown in Figure 1, can be explained by taking into account some blocking of reduction nuclei by adsorbed water, as it was found in the study on Fe_2O_3 reduction [2]. The strong quickening of the reduction velocity caused by enhancement of the heating rate can be connected with self-catalyzed nucleation, (autocatalysis) as the rate-determining step in a uniform internal reduction on the low-temperature side of the TPR peak. The observed induction period becomes more significant with decreasing reduction temperature.

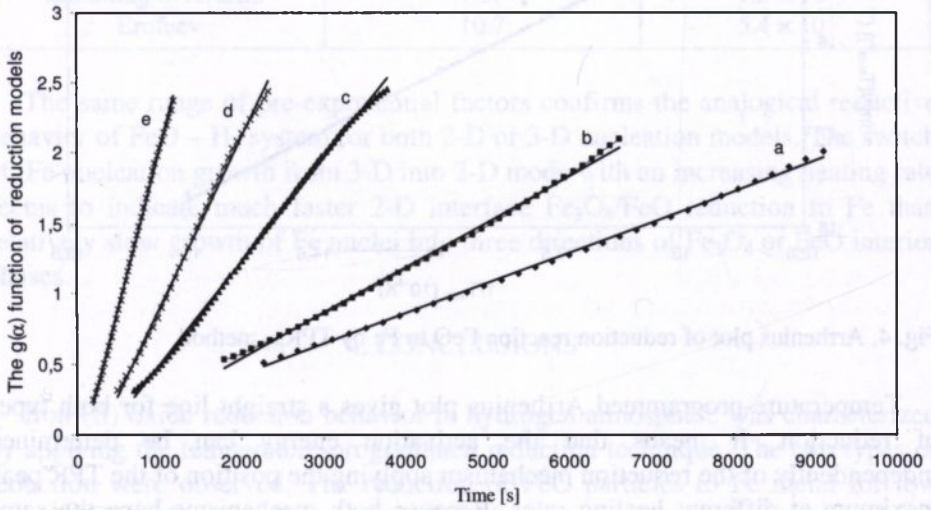

Fig. 3. Avrami-Erofeev's graphs of the g(α) function vs. time for the 3-D nucleation model for heating rates: φ = 0.58 °C/min – a, φ = 1.07 °C/min – b and 2-D nucleation model for: φ = 2.57 °C/min – c, φ = 5.52 °C/min – d, φ = 10.7 °C/min – e, respectively.

The findings are supported by literature [21-22], e.g. for the reduction of Fe_3O_4 at 200–580 °C [18,19]. Apparently, nuclei catalyze more nuclei formation, either due to branching of nuclei or to the catalytic role of Fe metal in H_2 dissociation. Water can aid during the acceleration by assuring hydrogen spillover process. Possibly, around the maximum of TPR peak according to the Avrami-Erofeev's model mechanism the explosive nuclei creation is completed and overlap of nuclei will begin. A crucial role in nuclei formation can be assigned to thermally activated FeO disproportionation (equation (c), not consuming hydrogen but providing uniformly distributed Fe^0 sites serving as nucleation sites of metallic iron phase formation in the interphase FeO/Fe_3O_4 region [18].

Figure 4 is the Arrhenius plot of FeO reduction which is plotted equation (2),

$$\ln(\frac{\varphi}{T_{max}^2}) = -\frac{E}{R \cdot T_{max}} - \ln(\frac{E}{A \cdot R}) + C \quad (2)$$

which is generalized Kissinger approach [2, 23].

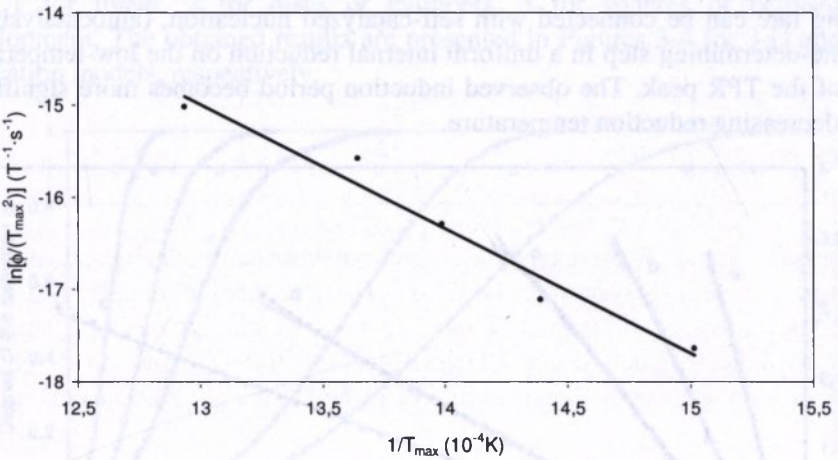

Fig. 4. Arrhenius plot of reduction reaction FeO to Fe by TPR_{H2} method.

Temperature-programmed Arrhenius plot gives a straight line for both types of reduction. It means that the activation energy can be determined independently of the reduction mechanism applying the position of the TPR peak maximum at different heating rates. Because both mechanisms have the same rate determining step-nuclei formation originating from FeO disproportionation, therefore the same apparent activation energies can be expected. And so, the activation energy of both reduction mechanisms calculated with slope-E/R has value 112 kJ/mol and as expected this value of FeO reduction to Fe is higher than analogical values of F_2O_3 reduction to Fe_3O_4 89 kJ/mol or Fe_3O_4 reduction to Fe 70 kJ/mol [12]. In the same way the lowering order of different iron oxide reducibility in hydrogen follows, $F_3O_4 > Fe_2O_3 > FeO$. Pre-exponential A values were calculated from equation (3) given by lit. [12]

$$A = -\frac{E}{RT_{max}^2} \cdot \frac{\varphi \cdot e^{\frac{E}{RT_{max}}}}{(\frac{df(\alpha)}{d\alpha})_{T=T_{max}}} \quad (3)$$

using both, the calculation values activation energy E, T_{max} and the differentiation of f(α) function of 3-D and 2-D model of Avrami-Errofeev from Table 1, then for $\alpha_{T=Tmax}$ calculated $df(\alpha)/d\alpha)_{T=Tmax}$ values.

Tab. 2. Calculated A values by using E=112 kJ/mol for the selected reduction models.

Reduction model	Heating rates, φ [°C/min]	A, [s^{-1}]
Three-dimensional nucleation according to Avarmi-Erofeev	0.58 1.07	4.0×10^5 3.2×10^5
Two-dimensional nucleation according to Avarmi-Erofeev	2.57 5.52 10.7	10.8×10^5 7.3×10^5 5.4×10^5

The same range of pre-exponential factors confirms the analogical reductive behavior of FeO – H_2 system for both 2-D or 3-D nucleation models. The switch of Fe nucleation growth from 3-D into 2-D mode with an increasing heating rate seems to indicate much faster 2-D interface Fe_3O_4/FeO reduction to Fe than relatively slow growth of Fe nuclei into three directions of Fe_3O_4 or FeO interior phases.

4. CONCLUSIONS

Iron (II) oxide reduction behavior in hydrogen atmosphere was characterized by applying the temperature-programmed reduction technique. The two types of reduction were observed. The reduction of FeO particles to Fe metal for low heating rates, that is 0.58 and 1.07 °C/min was shown to process with three-dimensional nucleation according to Avrami-Erofeev's model as the rate-determining step. This mechanism represents uniform internal reduction. The rate-determining step is probably self-catalyzed nucleation manifested upon the low-temperature side of the TPR peak. For higher heating rates, namely, 2.57, 5.52, 10.7 °C/min this reduction can be described by the two-dimensional nucleation of Avrami-Erofeev's model. The activation energy, E = 112 kJ/mol can be determined irrespective of the reduction mechanism, from the shift of the TPR peak maximum using different heating rates. The change of FeO reduction mechanism with the heating rate was assigned to the considerable contribution of temperature dependent FeO disproportionation resulting in Fe^0 atoms serving not only as nucleation sites of iron phase but also as chemisorption sites for hydrogen molecules. Depending on heating rate the apparently simple one-step reduction FeO → Fe can be treated as a much more complicated two-step process FeO → Fe_3O_4 → Fe up to 570 °C, or even a three-step process FeO →

$Fe_3O_4 \rightarrow FeO \rightarrow Fe$ above 570 °C. The existence of Fe_3O_4 and FeO as intermediates does not depend very much on the kind of starting iron oxide but mostly there are strongly dependent on temperature of reduction determining entirely the reduction mechanistic pathways.

Acknowledgements
The financial support of this work by the Polish Scientific Research Council supports (Grant No. 4T09 146 25) is gratefully acknowledged.

5. REFERENCES

[1] G. Muntenanu, L. Ilieva, D. Andreeva, *Thermochim. Acta* 291, 171 (1997).
[2] O.J. Wimmers, P. Arnoldy and J.A. Moulijn, *J. Phys. Chem.* 90, 1331 (1986).
[3] N.W. Hurst, S.J. Gentry, A. Jones, B.D. Mc Nicol, *Catal. Rev.* 24233 (1982).
[4] C. Li, Y.W. Chen, *Thermocim.Acta* 256, 457 (1995).
[5] Barański, J. Langan, A. Patek, A. Reizer, *Appl. Catal.* 3, 207 (1982).
[6] R. Brown, M.E. Copper, S.A. Whan, *Appl. Catal.* 3, 177 (1982).
[7] E.E. Unmuth, L.H. Schwartz, J.B. Butt, *J. Catal.* 63, 404 (1980).
[8] D.B. Bukur, X. Lang, J.A. Rossin, W.H. Zimmerman, M.P. Rosynek, C. Li, *Ind. Eng. Res.* 29, 1588 (1990).
[9] R.M. Cornel, U. Schwertman, *The Iron Oxides*, VCH Verlagsgesellschaft mbH, Weinheim 1996.
[10] D.A.M. Monti, A. Baker, *J. Catal.* 83, 323 (1983).
[11] P. Malet, A. Caballero, J. Chem., *Soc. Faraday Trans.* 84, 2369 (1988).
[12] H.Y. Lin, Y.W. Chen, Ch. Li, *Thermochim. Acta* 400, 61 (2003).
[13] W. Jander, *Angew. Chem* 41, 79 (1928).
[14] M. Avrami, *J. Chem. Phys.* 7, 1103 (1939).
[15] M. Avrami, *J. Chem. Phys.* 8, 212 (1940).
[16] M. Avrami, *J. Chem. Phys.* 9, 117 (1941).
[17] V. Erofeev, *Dokl. Acad. Sci. URSS*, 52515 (1946).
[18] W.K. Jóźwiak, E. Kaczmarek, T.P. Maniecki, W. Maniukiewicz, *Appl. Catal.* 326, 17 (2007).
[19] L.G. Harrison, in: *Comprehensive Chemical Kinetics*, C.H. Bamford, C.F.H. Tipper (Eds), vol. 2, Elsevier, Amsterdam 1969, p. 57.
[20] E.T. Turkdogan, J.V. Vinters, *Metall. Trans.* 3, 3175 (1971).
[21] M. Shimokawabe, R. Furuichi, T. Ishi, *Thermocim. Acta* 28, 287 (1979).
[22] M.V.C. Sastri, R.P. Viswanath, *Int. J. Hydrogen Energy* 7, 951 (1982).
[23] H.E. Kissinger, *Anal. Chem.* 29, 1702 (1957).